Reorientations of divacancies in silicon

R H van der Linde and C A J Ammerlaan
Natuurkundig Laboratorium, Universiteit van Amsterdam, Valckenierstraat 65,
1018 XE Amsterdam, The Netherlands

Abstract. Reorientations of negative divacancies are induced by linearly polarised infrared light with a wavelength of 3·6 μm, and by applying uniaxial stress. The orientations are observed directly in the Si-G7 EPR spectrum. The degree of alignment as a function of the direction of polarisation of the light has been studied. The characteristic time for the thermally activated anneal of this alignment is measured between 16 and 18·3 K, and is found to depend on the donor concentration; it has different values for the stress and the optically induced alignment.

1. Introduction

The EPR spectra Si-G6 and Si-G7 are associated with the single positive and the single negative charge states of the divacancy in silicon, respectively. The divacancy is an extensively studied defect (Watkins and Corbett 1965) and for convenience we shall summarise here some of its main properties.

The stereographic model in figure 1 shows a divacancy consisting of the two broken circles c and c′, surrounded by six labelled atoms. By removing the Si atoms c and c′ six broken bonds remain at the six labelled atoms. The electrons in the broken bonds will pair off in a symmetrical way as a manifestation of the Jahn–Teller effect, lowering the symmetry from $\bar{3}m$ (D_{3d}) to $2/m$ (C_{2h}). As a consequence of this low symmetry, the divacancy can be accommodated in the lattice in 12 spatially different orientations, which are labelled by two letters. The first letter specifies the direction of the second vacancy as seen from the vacancy site c′ in the centre of figure 1. (The letters ‘a’, ‘b’, ‘c’, ‘d’ define four ⟨111⟩ bond directions in the lattice.) The second letter denotes the atoms lying in the mirror plane of the divacancy, i.e. the atoms between which the extended bond is formed. So in figure 1 the orientation cb is shown. The extended bond may contain one, two, three or four electrons, depending on the position of the Fermi level. The states with one and three electrons are paramagnetic and give rise to the EPR spectra G6 and G7, respectively, with $S = 1/2$.

The low symmetry is reflected in the g tensor, which is shown in figure 2 for G7 when the external magnetic field **B** is chosen in the $(0\bar{1}1)$ plane. Because of this choice of **B** the directions ‘b’ and ‘c’ in figure 1 are equivalent, which is reflected in the labelling of the divacancies: letters b and c are interchangeable, the resonances are coincident. As can be seen from figure 2, two pairs of resonances (ab, ac) and (db, dc) almost coincide over the entire angular range. At K-band frequencies, these components cannot be resolved experimentally. Therefore, at most six discrete resonances can be discerned in practice. The best resolution is obtained with an angular setting of **B** of 27° off the [100] direction toward [011], indicated by the broken vertical line in figure 2.

0305–2346/79/0046–0242 $01.00

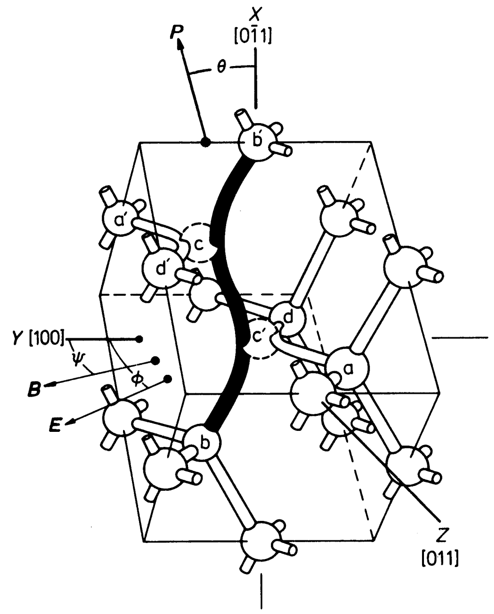

Figure 1. Model of the divacancy in silicon. Letters a, b, c, d denote ⟨111⟩ bond directions as seen from site c'. Broken circles c and c' represent vacancies. Defect orientation cb is shown. The extended bond is drawn heavily.

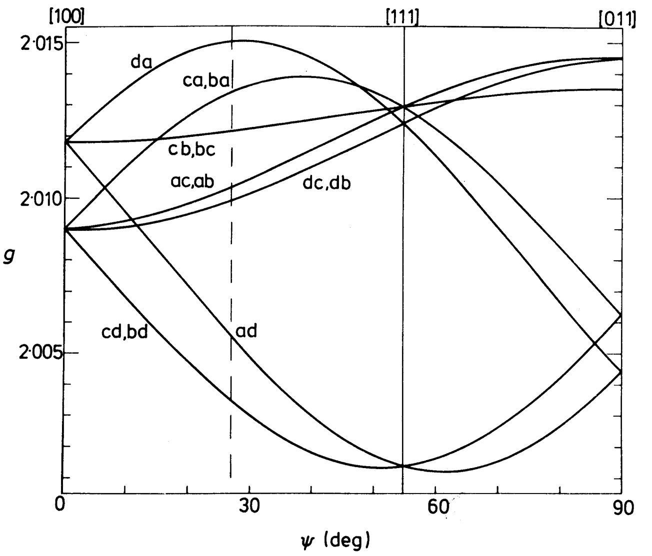

Figure 2. *g*-values as a function of crystalline orientation with **B** in the (0$\bar{1}$1) plane for the G7 spectrum of the negative divacancy in silicon. Curves are labelled with the corresponding defect orientations.

2. Experimental set-up

We studied the alignment and its annealing on two floating-zone samples containing different concentrations of phosphorus: sample I contained $10^{18}\,\mathrm{cm}^{-3}$, and sample II

$2\times10^{16}\,\mathrm{cm}^{-3}$. Divacancies were produced by bombardment with 1·5 MeV electrons at room temperature (up to 40 °C), the electron doses being: samples I, $3\times10^{18}\,\mathrm{cm}^{-2}$; and sample II, $2\times10^{18}\,\mathrm{cm}^{-2}$. The estimated (Corbett and Watkins 1965) divacancy concentrations are therefore $3\times10^{16}\,\mathrm{cm}^{-3}$ for sample I and $2\times10^{16}\,\mathrm{cm}^{-3}$ for sample II. Besides divacancies, the samples contain other defects. Some of them are paramagnetic before (G16, NL7), others (G8) only after illumination with light of the right wavelength. Of these, only G8 caused trouble, notably for wavelengths below 1·9 μm in sample I.

Samples were cut along a ⟨011⟩ direction and polished in an almost cylindrical shape with a diameter of 1·8 mm. They were mounted with their greatest dimension along the axis of a cylindrical TE_{011} K-band cavity, the top of the sample extending through a hole in the top of the cavity. Directly above the sample, a Brewster-angle polariser using a polished germanium wedge and three aluminium mirrors (Bor and Brooks 1966) could be mounted. The polariser could be rotated from the outside of the cryostat by a stainless-steel hollow pipe. Inside this pipe, a thin-walled 4·3 mm diameter silver tube is inserted to guide the light. A 36 μm mylar window was used at the entrance. Uniaxial stress was applied by replacing the light pipe and polariser by a stainless-steel rod to transmit force to the sample. The EPR spectra were taken with a superheterodyne K-band spectrometer tuned to dispersion.

Temperature was monitored by an Au(0·03% Fe)–chromel thermocouple mounted in the cavity wall and kept constant within 0·1 K. All spectra were taken at 8·8 K.

3. Results

Starting with a sample containing a uniform distribution of divacancies, a redistribution of divacancies has been obtained by shining linearly polarised near-infrared light on the sample. The redistribution is monitored directly in the EPR spectrum, an example being shown in figure 3. The total sum of the EPR resonance intensities is constant, demonstrating that no divacancies disappear or lose their paramagnetism. The alignment is clearly a result of electronic redistribution because the sum of the EPR intensities is also

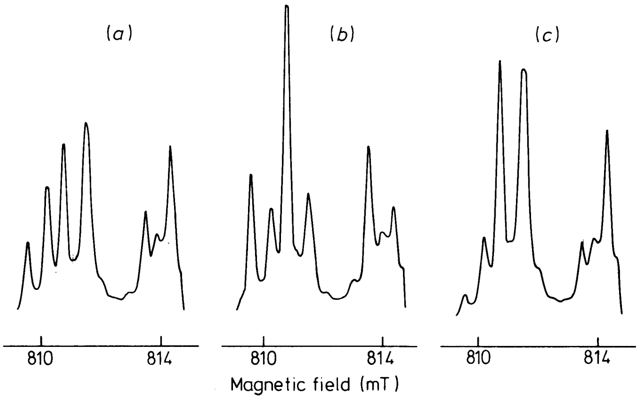

Figure 3. EPR spectra of the negative divacancy for **B** ∥ [100] + 27° in the (0$\bar{1}$1) plane at 8·8 K: (*a*) the spectrum before illumination; (*b*) after illumination, λ = 3·6 μm, **E** ∥ [100] + 8° in the (0$\bar{1}$1) plane; (*c*) similar to (*b*), but **E** ∥ [100] − 2·5°.

constant within each Jahn–Teller triplet (i.e. the vacancy–vacancy axis is preserved), as should be expected at such low temperatures.

In figure 4 the saturation values of the alignment are shown as a function of the direction of polarisation of the light, i.e. the direction of **E** in the $(0\bar{1}1)$ plane (see figure 1). These values are obtained by illuminating the sample at 8·8 K (or sometimes at 4·2 K, which gives the same results) for about 35 min and then taking the EPR spectrum in the dark. Before taking the next polarisation direction the sample was 'randomised' by heating it at about 30 K for a few seconds (cf figure 6).

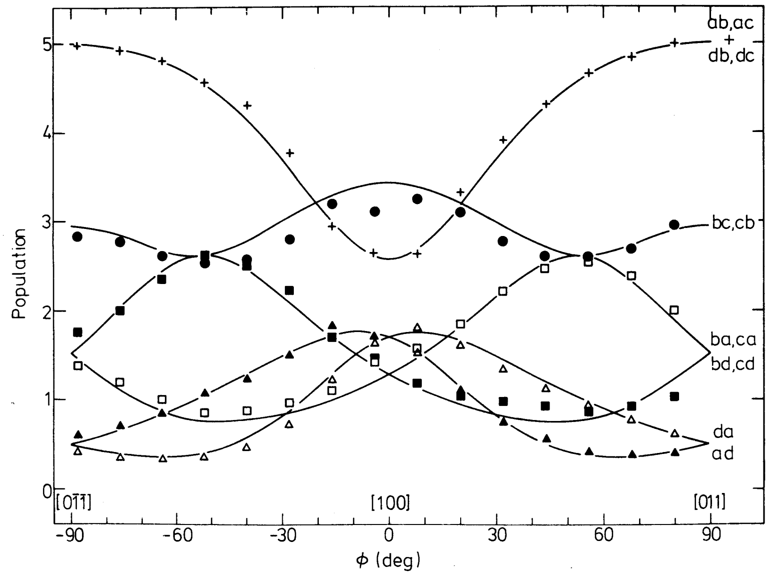

Figure 4. Saturation values of populations of the various divacancy orientations as a function of the direction of polarisation, with **E** in the $(0\bar{1}1)$ plane. Full curves are calculated for a transition with dipole moment in the reflection plane of the divacancy, angle $\theta = -2{\cdot}5°$.

Ammerlaan and Watkins (1972) performed an analogous experiment on the positive divacancy spectrum G6. Our effects are much larger (possibly because our degree of polarisation was higher) but exhibit about the same angular dependence. The full curves in figure 4 are calculated using their model but incorporating a parameter which accounts for the degree of polarisation. In our calculations we used an angle $\theta = -2{\cdot}5°$ for the direction of the dipole moment vector in the XY-plane of a particular divacancy orientation, to be compared with $\theta = +15°$ determined by Ammerlaan and Watkins (1972) for G6. It should be noted that the change of sign, in comparison with the latter reference, is a consequence of the different definition of the angle θ, as illustrated in figure 1. In order to eliminate the minus sign in the definition of $\tan\theta$ the angle θ is taken as positive from the $+X$-axis towards the $+Y$-axis.

The optimal alignment has been obtained with a wavelength of $3{\cdot}6 \pm 0{\cdot}2\,\mu$m. For $4{\cdot}0 < \lambda < 12\,\mu$m no effect could be detected; below $1{\cdot}9\,\mu$m the light generated other EPR spectra, mainly G8 and GGA1, at the expense of G7, which impeded the observations too much.

The alignment caused by uniaxial stress is well known (Watkins and Corbett 1965). We heated the sample to about 30 K under a stress of about 200 kg cm^{-2} along the [0$\bar{1}$1] direction, in order to create changes in population of the same order of magnitude as that obtained in the experiment with light. We studied the recovery of the alignment to a

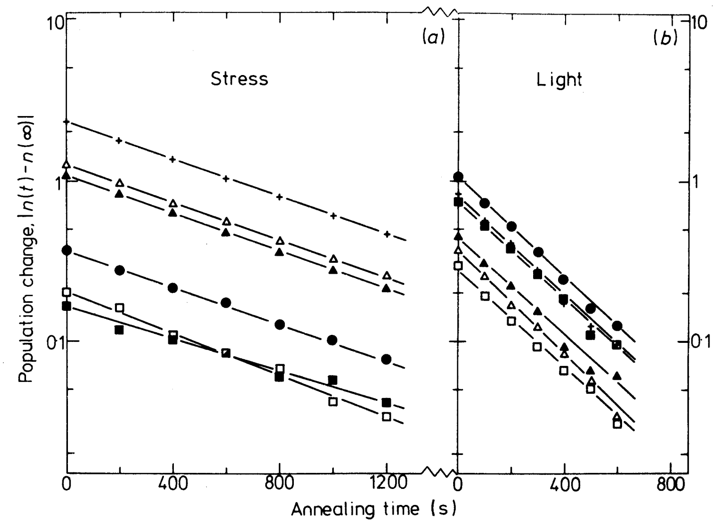

Figure 5. Isothermal anneal at 17·3 K of alignment by (*a*) uniaxial stress along [0$\bar{1}$1], and (*b*) polarised light, E ∥ [100] + 80°. Symbols are the same as those used in figure 4 for the various divacancy orientations.

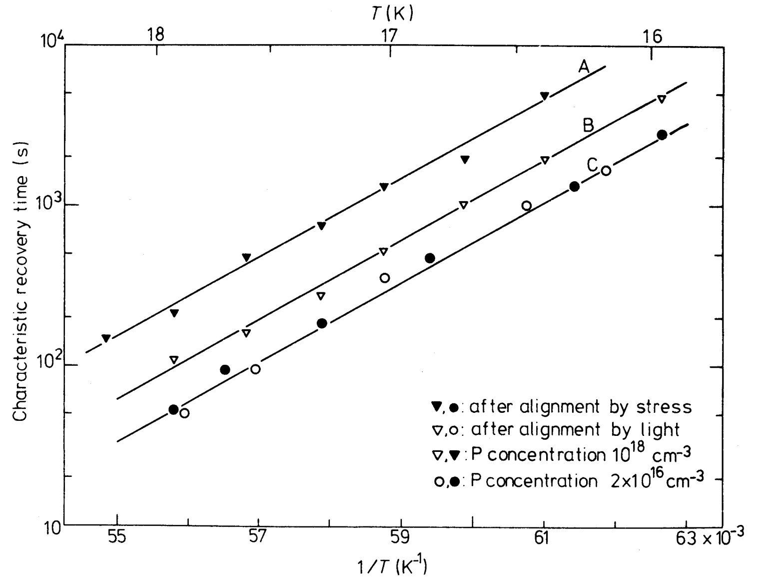

Figure 6. Characteristic recovery time as a function of the reciprocal temperature for sample I (lines A and B) and sample II (line C). The lines are fitted by $\tau^{-1} = \nu_0 \exp(-E/kT)$ where $E = 49$ meV for all three lines and ν_0 takes the values $\nu_0 = 2{\cdot}5 \times 10^{11}\,\mathrm{s}^{-1}$ (line A), $\nu_0 = 7{\cdot}5 \times 10^{11}\,\mathrm{s}^{-1}$ (line B) and $\nu_0 = 1{\cdot}5 \times 10^{12}\,\mathrm{s}^{-1}$ (line C).

random distribution in isothermal anneals in the temperature range 16–18·3 K after both methods of redistributing the divacancies. A typical example is shown in figure 5 for annealing at 17·3 K. Figure 5 (*a*) shows the recovery of the six EPR lines after alignment by stress in 200 s anneals, figure 5(*b*) shows the same after alignment by light for 100 s anneals. Both annealings are on the same sample I with the high phosphorus concentration.

It is immediately clear that recovery is much faster after the optically induced redistribution. It also can be seen that the different orientations recover at the same rate in each separate experiment. Sample II did not exhibit such differences between optically and stress-induced alignment. In this sample the recovery of each spectrum also follows a simple exponential law with a time constant depending on temperature. These characteristic recovery times are shown in figure 6 together with those obtained for sample I. The slope of the three lines corresponds to an activation energy of about 49 meV, which is somewhat lower than the 56 meV determined by Watkins and Corbett (1965). The value they found is much more accurate than our value, but at any rate the lifetime of the reorientation we determined is an order of magnitude smaller at 17 K. We do not have an explanation for this discrepancy. A possible explanation for the different recovery times after alignment by stress or light could be the fact that stress influences the whole crystal, containing many other defects in the neighbourhood of the divacancy, while the light only affects a defect having the right transition dipole moment in the right absorption band. The shorter recovery times in sample II seem to corroborate this explanation.

References

Ammerlaan C A J and Watkins G D 1972 *Phys. Rev.* B5 3988–93
Bor J and Brooks L A 1966 *J. Sci. Instrum.* 43 944
Corbett J W and Watkins G D 1965 *Phys. Rev.* 138 A555–60
Watkins G D and Corbett J W 1965 *Phys. Rev.* 138 A543–55